A New Family of Space/Wavelength/Time Spread Three-Dimensional Optical Code for OCDMA Networks

Sangin Kim, Kyungsik Yu, and Namkyoo Park, *Member, IEEE, Member, OSA*

***Abstract*—A new family of space/wavelength/time spread three-dimensional (3-D) optical codes for optical code-division multiple-access (OCDMA) networks has been proposed. Two types of 3-D codes have been constructed: 3-D codes with single pulse per plane and 3-D codes with multiple pulses per plane. Both codes are based on the prime sequence algorithm and have shown improved performance compared to the previously proposed two-dimensional (2-D) prime code. Effective implementation of the 3-D code has also been proposed. In order to eliminate the requirement of fiber ribbons and multiple star couplers in space/wavelength/time spread 3-D code based optical networks, a wavelength^2/time scheme has been suggested, in which the periodic property of an arrayed waveguide grating (AWG) is used. It has been shown that the system performance can be maximized for given resources with a proper choice of the wavelength^2/time scheme. Due to the improved performance of the 3-D code and the effective architecture of the wavelength^2/time scheme, the feasibility of the OCDMA network is much enhanced.**

***Index Terms*—Optical code division multiple access (OCDMA), optical networks, space/wavelength/time spread 3-D optical code, wavelength^2/time scheme.**

I. Introduction

As THE feasibility of optical access networks increases, optical code-division multiple-access (OCDMA) networks attract much attention and have been studied by a number of authors in that it does not require fast switching and provides bursty, concurrent, asynchronous communications. The main issue of the studies on the OCDMA networks is to devise a code set of good system performance. In unipolar optical code based OCDMA systems, the system performance is determined by the bandwidth efficiency of the optical codes which is closely related with the error probability behavior of the optical code in multiple user circumstance as well as the code set size dependence on the code length. For the OCDMA scheme to be more realistic, it is desired to devise an optical code that can accommodate a larger number of simultaneous users with a low error probability for a given code length.

Since the optical orthogonal codes (OOC) were proposed [1], several types of optical codes have been suggested. The OOC is a one-dimensional (1-D) collection of binary sequences. In a 1-D OCDMA system, one period of transmission clock is divided into a given number of small temporal segments, dubbed as time chips, and bit "1" is encoded with a number of optical pulses spread in the time chips. The OOC has the lowest out-of-phase autocorrelation and cross-correlation values among 1-D families [1]–[10]—both are equal to one. The limit of 1-D optical codes is that out-of-phase autocorrelation cannot be zero because there are multiple optical pulses within one period. The lower limit of out-of-phase autocorrelation in the 1-D codes is 1, and to achieve it as in the OOC, code length increases rapidly as the number of users increases. To overcome the limit of the 1-D optical codes, 2-D approaches are proposed [11]–[15]. In the 2-D optical codes, optical pulses are spread in both space and time domains [11], [12] or in wavelength and time domains [13]–[15]. By employing another dimension (space or wavelength), 2-D code with single pulse per row is achieved and the performance of the 2-D OCDMA system is much improved in comparison to the 1-D OCDMA system. Out-of-phase autocorrelation and cross-correlation of 2-D code families are equal to 0 and 1, respectively. The generalized algebraic algorithms of the 2-D code construction are the prime code [5], [6], [15] and the Reed–Solomon code [9], [10], [15], and both wavelength/time code and space/time code can be constructed by either of those algorithms. Besides the algebraic unipolar 2-D code-based OCDMA scheme, recently, the demonstration of the OCDMA system based on the periodic spectrum encoding has been reported [16].

With simple extension of the 2-D optical code, 3-D optical code in which optical pulses are spread in space, wavelength, and time domains can be easily constructed, and the performance is further improved. One simple approach is hybridizing the wavelength-division multiplexing (WDM) scheme with the space/time code based CDMA scheme, where the 2-D space/time codes is applied to each available wavelength independently [17], [19]. It has been shown that with the simple WDM–CDMA hybrid scheme, the bandwidth penalty of the 2-D space/time codes can be relaxed [17], [19]. Besides the simple approach, more sophisticated WDM–CDMA hybrid schemes, in which all available wavelengths are used in each codeword, have been suggested [18]–[21]. In the previous works [18]–[21], however, the cases where the same number of wavelengths as the spatial channels are used have been mainly considered, and generalized code generation algorithm has not been fully discussed. Therefore, the estimation of the code set size for generalized orthogonal codes was not given explicitly. Moreover, in the scheme that was referred to as the

Manuscript received July 23, 1999; revised December 8, 1999.

S. Kim is with Korea Telecom, Access Network Laboratory, Taejeon, Korea (e-mail: sangin@kt.co.kr).

K. Yu and N. Park are with Seoul National University, School of Electrical Engineering, Seoul 151-742, Korea (e-mail: nkpark@plaza.snu.ac.kr).

Publisher Item Identifier S 0733-8724(00)03043-7.

WDM matrix code in [18], loose (not minimal) cross-correlation constraint was imposed, and all possible ways ($n!$) of ordering n wavelengths were considered as codewords. Hence, as the number of wavelengths (n) increases, the maximum cross-correlation value of the code increases ($n-2$).

In this paper, we propose generalized space/wavelength/time spread 3-D optical orthogonal codes having 0 out-of-phase autocorrelation and 1 cross-correlation values. The algebraic generation algorithm of the 3-D codes is discussed explicitly and the orthogonality of the proposed 3-D codes is proven mathematically. The proposed 3-D code generation algorithm is generalization and extension of the previous hybrid schemes with the stringent out-of-phase autocorrelation and cross-correlation constraints imposed. The performance of the proposed 3-D codes is analyzed in comparison with that of the 2-D codes. Physical implementation of the 3-D code is also considered, and it is shown that the proposed 3-D code can be realized with incoherent broadband light sources in wavelength^2/time form by utilizing the periodic property of an arrayed waveguide grating (AWG) [22] eliminating the requirement of fiber ribbons and multiple star couplers in networks.

The last part of the paper is organized as follows. Some frequently used notations and basic concepts are defined in Section II. In Section III, the 2-D prime code is briefly reviewed, and in Section IV, construction of the 3-D code is described. The performance of the proposed 3-D code is analyzed and compared with the 2-D code in Section V. In Section VI, implementation of the 3-D code and newly proposed wavelength^2/time scheme are discussed. Brief concluding remarks are given in Section VII.

II. Preliminaries

Codewords of three-dimensional (3-D) code are represented by 3-D matrices that have binary (1 or 0) values for their elements. For the 3-D code expanded over space, wavelength, and time domains consists of $S \times W \times T$ matrices where S, W, and T denote the numbers of spatial channels, wavelengths, and time chips, respectively. Each element represents whether the corresponding point in 3-D conceptual space is occupied by an optical pulse or not. The fact that (s, w, t) element of the matrix is equal to 1 means an optical pulse of wavelength w exists at time chip t in spatial channel s.

In networks based on the space/wavelength/time 3-D code, every user is assigned a codeword matrix as its own address signature. A user transmits data bit "1" with a sequence of pulses spread in the space, wavelength, and time domains according to the code matrix of its intended receiver. At the receivers, the pulses of different spatial channels are separated and in each spatial channel, the pulses of each wavelength are correlated separately in the time domain. After correlation, all pulses are collected together. Only at the intended receiver, all the spread pulses are assembled in the same time chip and one large optical pulse is obtained, which is dubbed as the autocorrelation function. Whereas, at other receivers, a series of small pulses are obtained, which is dubbed as the cross-correlation function. Then, the data bit "1" can be recovered by threshold-detecting the peak of the optical pulse. Data bit "0" is implemented by transmitting nothing.

Now, we define the 3-D code in mathematical language.

Definition: A ($l \times m \times n$, c_w, λ_a, λ_c) 3-D code, C, is a collection of binary (0, 1) $l \times m \times n$ matrices, each of Hamming weight c_w, such that the following constraints are satisfied.

- *Autocorrelation Constraint*: For any 3-D codeword $X \in C$

$$\sum_{i=0}^{l-1}\sum_{j=0}^{m-1}\sum_{k=0}^{n-1} x_{i,j,k}x_{i,j,k\ominus\tau} = c_w \qquad \text{for } \tau = 0$$
$$\leq \lambda_a \qquad \text{for } 1 \leq \tau \leq n-1 \tag{1}$$

  where

$x_{I,j,k} \in \{0, 1\}$	is an element of matrix X;
c_w	is the code weight;
a nonnegative integer, λ_a	is out-of phase autocorrelation;
$\oplus$	denotes modulo-n addition.

- *Cross-Correlation Constraint*: For any two distinct 3-D codewords $X, Y \in C$

$$\sum_{i=0}^{l-1}\sum_{j=0}^{m-1}\sum_{k=0}^{n-1} x_{i,j,k}y_{i,j,k\ominus\tau} \leq \lambda_c \qquad \text{for } 0 \leq \tau \leq n-1 \tag{2}$$

  where $x_{I,j,k}$, $y_{I,j,k} \in \{0, 1\}$ are elements of matrices X and Y, respectively, and a nonnegative integer, λ_c is cross-correlation.

The cross-correlation constraint guarantees asynchronous operation of the 3-D code-based system. A ($m \times n$, c_w, λ_a, λ_c) 2-D code can be defined similarly just by replacing $l \times m \times n$ matrices with $m \times n$ matrices in the above definition [15].

In this paper, for visualization of a 3-D codeword, $l \times m \times n$ matrix, we form a stack of $m \times n$ matrices as depicted in Fig. 1 and we call each $m \times n$ matrix a plane.

III. 2-D Code Construction

The basic idea of constructing a 2-D code is to assign temporal locations (time chips) of optical pulses to each spatial channel (or wavelength) in such a way that for any two distinct codewords, there is a coincidence of optical pulses only at one spatial channel (or wavelength). Otherwise, cross-correlation of the code will be higher than 1. To guarantee zero out-of-phase autocorrelation, all pulses should be assigned to different spatial channels (or different wavelengths), which is equivalent to the codeword matrices having only one "1" in each row. In other words, the code should have single pulse per row.

2-D codes can be constructed by modifying 1-D prime codes and 1-D Reed–Solomon codes [15]. The author of [15] called them generalized multiwavelength prime codes (GMWPC's) and generalized multiwavelength Reed–Solomon codes (GMWRSC's). They are named assuming that they are to be used for wavelength/time codes, but they can be directly applied to construct space/time codes. In this paper, we will call them 2-D prime codes and 2-D Reed–Solomon codes, respectively, not restricting their application to wavelength/time

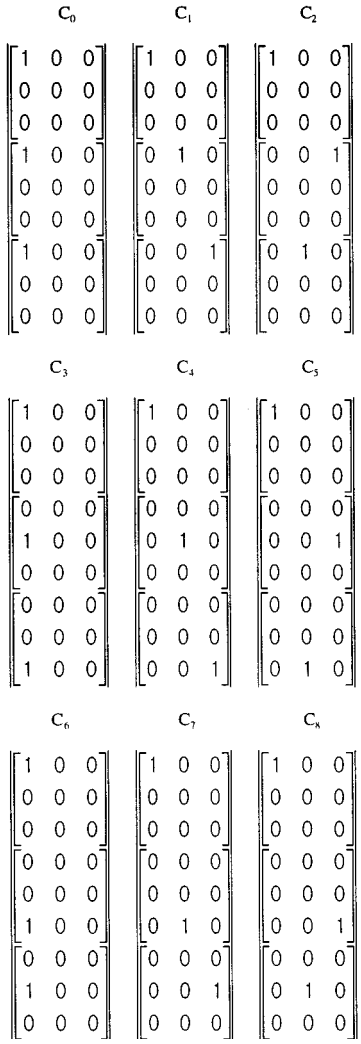

Fig. 1. Visualization of 3 × 3 × 3 matrices. Each stack of 3 × 3 matrices represents a codewords of (3 × 3 × 3, 3, 0, 1) 3-D code. Each column and row of 3 × 3 matrices represent a time chip and a wavelength, respectively. Each 3 × 3 matrix represents a spatial channel or wavelength/time plane.

codes. Since we focus on 3-D code construction based on the prime code construction algorithm in this paper, only the 2-D prime code is considered in this section. The 2-D prime code algorithm is presented in mathematical language as follows.

Given integers S and $T = p_1 p_2 \cdots p_k$ for a set of prime numbers such that $p_k \geq p_{k-1} \geq \cdots \geq p_1 \geq S$, the ($S \times T$, S, 0, 1) code is represented by $S \times T$ matrix $X(i_1, i_2, \cdots, i_k)$ whose element $x_{s,t}$ is given by

$$\begin{aligned} &x_{s,t}(i_1, i_2, \cdots, i_k) = 1 \\ &\quad \text{for } t = s \otimes_{p_1} i_1 + (s \otimes_{p_2} i_2)p_1 \\ &\qquad + \cdots + (s \otimes_{p_k} i_k)p_1 p_2 \cdots p_{k-1} \\ &x_{s,t}(i_1, i_2, \cdots, i_k) = 0 \\ &\quad \text{for other } t \end{aligned} \tag{3}$$

for $s \in [0, S-1]$, $i_q \in [0, p_q - 1]$ $(q = 1, 2, \cdots, k)$, where $\otimes_p$ denotes modulo-p multiplication. The code has T codewords. The proof of zero out-of-phase autocorrelation and 1 cross-correlation is omitted in this paper, which is found in [15]. Similar proof will be given in the next section.

IV. 3-D Code Construction

Space/wavelength/time 3-D codes can be constructed by extending 2-D codes—space/time codes or wavelength/time codes. Let us assume $(S \times T, S, 0, 1)$ space/time 2-D codes. If multiwavelength light sources (W) are available for each spatial channel, we have another degree of freedom to choose the wavelength of each spatial channel in code construction. For a given temporal distribution of pulses over spatial channels, i.e., one codeword of the space/time 2-D code, many different codewords can be generated by changing the wavelength of pulse in each spatial channel. In assigning wavelength to each spatial channel, we need to keep the orthogonality by constraining cross-correlation between any two codewords with different temporal distributions of pulses over spatial channels less than or equal to 1. Note that cross-correlation between any two codewords with the same temporal distribution cannot be greater than 1 because of the orthogonality of the 2-D code. To extend 2-D codes to 3-D codes without losing orthogonality, we only need to assign wavelengths to each spatial channel such a way that any two distinct codewords have no more than one spatial channel of the same wavelength. To do so, we can employ the same algorithm that is used to assign temporal locations of pulses over spatial channels in construction of the 2-D code as given in Section III. In other words, we can construct space/wavelength/time 3-D code by applying 2-D construction algorithm separately to space/wavelength plane and space/time plane. The algorithms applied to space/time plane and space/wavelength plane can be different from each other. For example, the prime sequence algorithm for space/wavelength and the Reed–Solomon algorithm for space/time can be employed. In this paper, we only consider the case where the prime code algorithm is employed for those two planes.

We can generate W distinct codewords for each temporal distribution of pulses over space channels by applying the 2-D prime code algorithm for assigning W wavelengths over spatial channels. Fig. 1 shows 9 codewords in (3 × 3 × 3, 3, 0, 1) 3-D code constructed by employing the prime code algorithm, where C_3 and C_6 are generated from C_0 by assigning wavelengths to spatial channels in different ways with the same allocation of optical pulses in time. Moreover, if the number of wavelength is greater than or equal to that of spatial channels ($W \geq S$), due to the orthogonality of the 2-D prime code construction algorithm, every cyclic shift in wavelength domain also generates another codeword that is orthogonal to others. [You can verify this for the codewords shown in Fig. 1. Each codeword will generate two more codewords by shifting pulses in wavelengths. Consequently, we have 27 codewords in (3 × 3 × 3, 3, 0, 1) 3-D prime code.] Therefore, we can generate W^2T codewords by extending ($S \times T$, S, 0, 1) code to ($S \times W \times T$, S, 0, 1) code if $W \geq S$. If $W < S$, cyclic shift of codewords in wavelength domain coincide with other codewords, and thus, we have WT codewords for ($S \times W \times T$, S, 0, 1) 3-D code.

So far, we have assumed keeping the number of total pulses in a codeword equal to that of the 2-D code in construction of 3-D code by extending 2-D code. In this case, the 3-D code has one pulse per spatial channel, that is, single pulse per wavelength/time plane. Using the notation defined in Section II, ($S \times T$, S, 0, 1) 2-D code is extended to ($S \times W \times T$, S, 0, 1) 3-D code.

However, due to increased degree of freedom, we can also increase the number of pulses per spatial channel in the 3-D code satisfying orthogonality. In other words, 3-D code with multiple pulses per wavelength/time plane is possible. To satisfy the zero out-of-phase autocorrelation constraint, the number of pulses per plane should not be greater than that of available wavelengths. That is the only constraint on the number of pulses per wavelength/time plane. In our work, only the case where all available wavelengths are used for each wavelength/time plane is considered for 3-D code with multiple pulses per plane, i.e., $(S\times W\times T, SW, 0, 1)$. In such a case, we have SW space/wavelength channels, and to satisfy orthogonality, we need to allocate SW pulses in such a way that for any two distinct codewords there is a coincidence of optical pulses only in one space/wavelength plane. Then, construction of the $(S\times W\times T, SW, 0, 1)$ 3-D code is equivalent to construction of $(SW\times T, SW, 0, 1)$ 2-D code. To construct the $(S\times W\times T, SW, 0, 1)$ 3-D code by using the prime code algorithm, all the possible combinations of spatial channels and wavelengths are indexed with integers between 0 and $SW-1$ by mapping (s, w) to $j = sW + w$ ($s \in [0, S-1]$, $w \in [0, W-1]$), and $(SW\times T, SW, 0, 1)$ 2-D code, i.e., $SW\times T$ matrices $X_{\text{2-D}}$, is constructed applying the algorithms described in Section III. Then, 3-D codewords, i.e., $S\times W\times T$ matrices $X_{\text{3-D}}$, are obtained by remapping $x_{\text{2-D},\,j,\,t}$ to $x_{\text{3-D},\,s,\,w,\,t}$ [$s = (j - j \bmod W)/W$, $w = j \bmod W$], where x is an element of X.

In the last of this section, the construction algorithms of the 3-D code with single pulse per plane (w/SPP) and 3-D code with multiple pulses per plane (w/MPP) which were described above are presented in mathematical language.

A. 3-D Code w/SPP

1) Case 1—$W \geq S$, $T \geq S$: Given integers S, $W = q_1q_2\cdots q_m$, and $T = p_1p_2\cdots p_k$ for two sets of prime numbers such that $q_m \geq q_{m-1} \geq \cdots \geq q_1 \geq S$, $p_k \geq p_{k-1} \geq \cdots \geq p_1 \geq S$, the $(S\times W\times T, S, 0, 1)$ code is represented by $S\times W\times T$ matrix $X(h_1, h_2, \cdots, h_{m+1}, i_1, i_2, \cdots, i_k)$ whose element $x_{s,\,w,\,t}$ is given by

$$\begin{aligned}
&x_{s,\,w,\,t}(h_1, h_2, \cdots, h_{m+1}, i_1, i_2, \cdots, i_k) = 1\\
&\quad \text{for } w = s\otimes_{q_1} h_1 + (s\otimes_{q_2} h_2)q_1\\
&\qquad\qquad + \cdots + (s\otimes_{q_k} h_m)q_1q_2\cdots q_{m-1}) \oplus_W h_{m+1},\\
&\quad \text{and } t = s\otimes_{p_1} i_1 + (s\otimes_{p_2} i_2)p_1\\
&\qquad\qquad + \cdots + (s\otimes_{p_k} i_k)p_1p_2\cdots p_{k-1}\\
&x_{s,\,w,\,t}(h_1, h_2, \cdots, h_{m+1}, i_1, i_2, \cdots, i_k) = 0\\
&\quad \text{for } w,\ t
\end{aligned} \tag{4}$$

for $s \in [0, S-1]$, $h_j \in [0, q_j-1]$ $(j = 1, 2, \cdots, m)$, $h_{m+1} \in [0, W-1]$, and $i_n \in [0, p_n-1]$ $(n = 1, 2, \cdots, k)$. The operation, $\otimes_p$ represents modulo-p multiplication. The code has W^2T codewords. The term "$\oplus_W h_{m+1}$" represents the cyclic shift of pulses in wavelength domain. Since all the pulses belong to different spatial channels, zero out-of-phase autocorrelation constraint is clearly met. The cross-correlation constraint is proven as follows.

Proof: For any two distinct matrices $X(h_1, h_2, \cdots, h_{m+1}, i_1, i_2, \cdots, i_k)$ and $X(h'_1, h'_2, \cdots, h'_{m+1}, i'_1, i'_2, \cdots, i'_k)$, if cross-correlation is greater than 1, we have at least two coincidence of pulses of the same spatial channel and wavelength in any cyclic r shift of the matrices in time, which means following four equations are simultaneously satisfied for $s_1, s_2 \in [0, S-1]$ $(s_1 \neq s_2)$:

$$\begin{aligned}
&s_1\otimes_{q_1} h_1 + (s_1\otimes_{q_2} h_2)q_1\\
&\qquad + \cdots + (s_1\otimes_{q_k} h_m)q_1q_2\cdots q_{m-1}) \oplus_W h_{m+1}\\
&\quad = s_1\otimes_{q_1} h'_1 + (s_1\otimes_{q_2} h'_2)q_1\\
&\qquad + \cdots + (s_1\otimes_{q_k} h'_m)q_1q_2\cdots q_{m-1}) \oplus_W h'_{m+1}
\end{aligned} \tag{5}$$

$$\begin{aligned}
&s_1\otimes_{p_1} i_1 + (s_1\otimes_{p_2} i_2)p_1\\
&\qquad + \cdots + (s_1\otimes_{p_k} i_k)p_1p_2\cdots p_{k-1} + r\\
&\quad = s_1\otimes_{p_1} i'_1 + (s_1\otimes_{p_2} i'_2)p_1\\
&\qquad + \cdots + (s_1\otimes_{p_k} i'_k)p_1p_2\cdots p_{k-1}
\end{aligned} \tag{6}$$

$$\begin{aligned}
&s_2\otimes_{q_1} h_1 + (s_2\otimes_{q_2} h_2)q_1\\
&\qquad + \cdots + (s_2\otimes_{q_k} h_m)q_1q_2\cdots q_{m-1}) \oplus_W h_{m+1}\\
&\quad = s_2\otimes_{q_1} h'_1 + (s_2\otimes_{q_2} h'_2)q_1\\
&\qquad + \cdots + (s_2\otimes_{q_k} h'_m)q_1q_2\cdots q_{m-1}) \oplus_W h'_{m+1}
\end{aligned} \tag{7}$$

$$\begin{aligned}
&s_2\otimes_{p_1} i_1 + (s_2\otimes_{p_2} i_2)p_1\\
&\qquad + \cdots + (s_2\otimes_{p_k} i_k)p_1p_2\cdots p_{k-1} + r\\
&\quad = s_2\otimes_{p_1} i'_1 + (s_2\otimes_{p_2} i'_2)p_1\\
&\qquad + \cdots + (s_2\otimes_{p_k} i'_k)p_1p_2\cdots p_{k-1}.
\end{aligned} \tag{8}$$

Subtracting (7) from (5), we obtain

$$\begin{aligned}
&(s_1 - s_2)\otimes_{q_1} (h_1 - h'_1) + ((s_1 - s_2)\otimes_{q_2} (h_2 - h'_2))q_1\\
&\quad + \cdots + ((s_1 - s_2)\otimes_{q_k} (h_m - h'_m))q_1q_2\cdots q_{m-1} = 0.
\end{aligned} \tag{9}$$

Since $s_1 \neq s_2$, (9) is valid only when $h_n = h'_n$ for $n \in [1, m]$. If we substitute $h_n = h'_n$ for $n \in [1, m]$ into (5), we obtain $h_{m+1} = h'_{m+1}$. Similarly, subtracting (8) from (6), we obtain

$$\begin{aligned}
&(s_1 - s_2)\otimes_{p_1} (i_1 - i'_1) + ((s_1 - s_2)\otimes_{p_2} (i_2 - i'_2))p_1\\
&\quad + \cdots + ((s_1 - s_2)\otimes_{p_k} (i_k - i'_k))p_1p_2\cdots p_{k-1} = 0.
\end{aligned} \tag{10}$$

Since $s_1 \neq s_2$, (10) is valid only when $i_j = i'_j$ for $j \in [1, k]$. As a result, the assumption $X(h_1, h_2, \cdots, h_{m+1}, i_1, i_2, \cdots, i_k) \neq X(h'_1, h'_2, \cdots, h'_{m+1}, i'_1, i'_2, \cdots, i'_k)$ is violated. Therefore, cross-correlation cannot be greater than 1.

2) Case 2—$W < S$, $T \geq S$: Given integers S, W, and $T = p_1p_2\cdots p_k$ for a set of prime numbers such that $p_k \geq p_{k-1} \geq \cdots \geq p_1 \geq S$, the $(S\times W\times T, S, 0, 1)$ code is represented by $S\times W\times T$ matrix $X(h_1, i_1, i_2, \cdots, i_k)$ whose element $x_{s,\,w,\,t}$ is given by

$$\begin{aligned}
&x_{s,\,w,\,t}(h_1, i_1, i_2, \cdots, i_k) = 1\\
&\quad \text{for } w = h_1,\\
&\qquad t = s\otimes_{p_1} i_1 + (s\otimes_{p_2} i_2)p_1\\
&\qquad\qquad + \cdots + (s\otimes_{p_k} i_k)p_1p_2\cdots p_{k-1}\\
&x_{s,\,w,\,t}(h_1, i_1, i_2, \cdots, i_k) = 0\\
&\quad \text{for other } w,\ t
\end{aligned} \tag{11}$$

for $s \in [0, S-1]$, $h_1 \in [0, W-1]$, and $i_n \in [0, p_n - 1]$ $(n = 1, 2, \cdots, k)$. The code has WT codewords. Since all the pulses belong to different spatial channels, it is clear that out-of-phase autocorrelation is equal to 0. Actually, Case 2 can be understood as a subset of Case 1. If we set $h_n = 0$ for $n \in [1, m]$ in (4), we obtain the equations of the same form with (11). The proof of 1 cross-correlation constraint of the code is similar to that for the Case 1.

Proof: For any two distinct matrices $X(h_1, i_1, i_2, \cdots, i_k)$ and $X(h_1', i_1', i_2', \cdots, i_k')$, if cross-correlation is greater than 1, we have at least two coincidence of pulses of the same spatial channel and wavelength in any cyclic r shift of the matrices in time, which means following equations are simultaneously satisfied for $s_1, s_2 \in [0, S-1]$ $(s_1 \neq s_2)$

$$h_1 = h_1' \tag{12}$$

$$\begin{aligned} &s_1 \otimes_{p_1} i_1 + (s_1 \otimes_{p_2} i_2)p_1 \\ &\quad + \cdots + (s_1 \otimes_{p_k} i_k)p_1p_2\cdots p_{k-1} + r \\ &= s_1 \otimes_{p_1} i_1' + (s_1 \otimes_{p_2} i_2')p_1 \\ &\quad + \cdots + (s_1 \otimes_{p_k} i_k')p_1p_2\cdots p_{k-1} \end{aligned} \tag{13}$$

$$\begin{aligned} &s_2 \otimes_{p_1} i_1 + (s_2 \otimes_{p_2} i_2)p_1 \\ &\quad + \cdots + (s_2 \otimes_{p_k} i_k)p_1p_2\cdots p_{k-1} + r \\ &= s_2 \otimes_{p_1} i_1' + (s_2 \otimes_{p_2} i_2')p_1 \\ &\quad + \cdots + (s_2 \otimes_{p_k} i_k')p_1p_2\cdots p_{k-1}. \end{aligned} \tag{14}$$

Subtracting (14) from (13), we obtain

$$\begin{aligned} &(s_1 - s_2) \otimes_{p_1} (i_1 - i_1') + ((s_1 - s_2) \otimes_{p_2} (i_2 - i_2'))p_1 \\ &\quad + \cdots + ((s_1 - s_2) \otimes_{p_k} (i_k - i_k'))p_1p_2\cdots p_{k-1} = 0. \end{aligned} \tag{15}$$

Since $s_1 \neq s_2$, (15) is valid only when $i_j = i_j'$ for $j \in [1, k]$. As a result, the assumption $X(h_1, i_1, i_2, \cdots, i_k) \neq X(h_1', i_1', i_2', \cdots, i_k')$ is violated. Therefore, cross-correlation cannot be greater than 1.

B. 3-D Code w/MPP

Given integers S, W, and $T = p_1p_2\cdots p_k$ for a set of prime numbers such that $p_k \geq p_{k-1} \geq \cdots \geq p_1 \geq SW$, the $(S \times W \times T, SW, 0, 1)$ code is represented by $S \times W \times T$ matrix $X(i_1, i_2, \cdots, i_k)$ whose element $x_{s,w,t}$ is given by

$$\begin{aligned} &x_{s,w,t}(i_1, i_2, \cdots, i_k) = 1 \\ &\quad \text{for } t = (sW + w) \otimes_{p_1} i_1 + ((sW + w) \otimes_{p_2} i_2)p_1 \\ &\qquad + \cdots + ((sW + w) \otimes_{p_k} i_k)p_1p_2\cdots p_{k-1} \\ &x_{s,w,t}(i_1, i_2, \cdots, i_k) = 0 \\ &\quad \text{for other } t \end{aligned} \tag{16}$$

for $s \in [0, S-1]$, $w \in [0, W-1]$, and $i_n \in [0, p_n - 1]$ $(n = 1, 2, \cdots, k)$. The code has T codewords. Since all the pulses have different combinations of spatial channel and wavelength, i.e., belong to different space/wavelength channels, it is clear that out-of-phase autocorrelation is equal to 0. The cross-correlation constraint is proven as follows.

Proof: For any two distinct matrices $X(i_1, i_2, \cdots, i_k)$ and $X(i_1', i_2', \cdots, i_k')$, if cross-correlation is greater than 1, we have at least two coincidence of pulses of the same spatial channel and wavelength in any cyclic r shift of the matrices in time, which means following equations are simultaneously satisfied for $j_1 = s_1W + w$, $j_2 = s_2W + w (s_1 \neq s_2, j_1 \neq j_2)$, where s_1 and $s_2 \in [0, S-1]$, $w \in [0, W-1]$

$$\begin{aligned} &j_1 \otimes_{p_1} i_1 + (j_1 \otimes_{p_2} i_2)p_1 \\ &\quad + \cdots + (j_1 \otimes_{p_k} i_k)p_1p_2\cdots p_{k-1} + r \\ &= j_1 \otimes_{p_1} i_1' + (j_1 \otimes_{p_2} i_2')p_1 \\ &\quad + \cdots + (j_1 \otimes_{p_k} i_k')p_1p_2\cdots p_{k-1} \end{aligned} \tag{17}$$

$$\begin{aligned} &j_2 \otimes_{p_1} i_1 + (j_2 \otimes_{p_2} i_2)p_1 \\ &\quad + \cdots + (j_2 \otimes_{p_k} i_k)p_1p_2\cdots p_{k-1} + r \\ &= j_2 \otimes_{p_1} i_1' + (j_2 \otimes_{p_2} i_2')p_1 \\ &\quad + \cdots + (j_2 \otimes_{p_k} i_k')p_1p_2\cdots p_{k-1}. \end{aligned} \tag{18}$$

Subtracting (18) from (17), we obtain

$$\begin{aligned} &(j_1 - j_2) \otimes_{p_1} (i_1 - i_1') + ((j_1 - j_2) \otimes_{p_2} (i_2 - i_2'))p_1 \\ &\quad + \cdots + ((j_1 - j_2) \otimes_{p_k} (i_k - i_k'))p_1p_2\cdots p_{k-1} = 0. \end{aligned} \tag{19}$$

Since $j_1 \neq j_2$, (19) is valid only when $i_n = i_n'$ for $n \in [1, k]$. As a result, the assumption $X(i_1, i_2, \cdots, i_k) \neq X(i_1', i_2', \cdots, i_k')$ is violated. Therefore, cross-correlation cannot be greater than 1.

V. Performance Analysis

In this section, we analyze the performance of the optical codes discussed in the previous sections, the 2-D prime code, the 3-D code w/SPP, and the 3-D code w/MPP in respects of code set size, bandwidth efficiency, error probability in multiple user circumstance, and system scalability. For the comparison of the 3-D codes with 2-D codes, only the 2-D prime code is considered in this paper because direct comparison is possible for given resources. However, comparing only with the 2-D prime code among other 2-D approaches to demonstrate the performance improvement of the 3-D codes over the 2-D codes is justified in that the 2-D prime code is asymptotically optimal in the aspect of the cardinality and has performance comparable with the 2-D OOC and the 2-D Reed–Solomon code [15].

A. Code Set Size, Code Length, and Bandwidth Efficiency

With S spatial channels, W wavelengths, and T time chips (code length), we can construct WT (if $S > W$) or W^2T (if $S \leq W$) orthogonal codewords for the 3-D code w/SPP. Whereas, T orthogonal codewords can be constructed for the 2-D prime code and the 3-D code w/MPP. For a fixed code length, the code set size of the 3-D code w/SPP is larger than that of the 2-D prime code and the 3-D code w/MPP. This feature is very important in the aspect of the bandwidth efficiency of the system [11], [13], [17]–[21]. In an OCDMA system with a given modulation bandwidth of the light source, B_{source}, per-user bandwidth, B_{user}, is inversely proportional to the code length, that is, $B_{\text{user}} = B_{\text{source}}/T$ assuming that

the chip time is equal to the FWHM of the optical pulse. In the system based on the 2-D codes and the 3-D code w/MPP, the per-user bandwidth should be compromised with the number of total users (code set size). Whereas, for the 3-D code w/SPP, the code set size can be increased without reducing the per-user bandwidth. In other words, for the system based on the 2-D prime code and the 3-D code w/MPP to accommodate the same number of total users with the 3-D code w/SPP, the per-user bandwidth of the system need to be reduced.

According to the above discussion, it appears that the 3-D code w/MPP shows no improvement compared with the 2-D prime code in terns of bandwidth efficiency. In practice, however, the number of users who can access the network simultaneously with a guaranteed error probability is a more meaningful measure of the system performance rather than the number of total users, and thus, the bandwidth efficiency considering the number of simultaneous users is more important than that considering the number of total users. Therefore, the per-user bandwidths of codes to accommodate the same number of simultaneous users need to be considered. The number of simultaneous users is closely related with the error probability behavior of the codes in multiple user circumstance, which is discussed in detail in the following subsection. The bandwidth efficiency considering the number of simultaneous users is also discussed in the following subsection.

B. Error Probability in Multiple User Circumstance

Now, we analyze the error probability behavior of the 2-D prime codes and the 3-D codes. In the analysis of the error probability of the OCDMA system, we ignore thermal and shot noises in photodetection, and only the interference from other users is considered. We also assume that there is either complete overlap of chips or no overlap when two codewords are correlated—chip synchronization—for the sake of mathematical convenience [12], [15]. Note that this does not mean that the system is synchronous and the chip synchronization assumption is different from the "bit synchronization" as in synchronous systems. We are still dealing with asynchronous systems without system clock and it has been shown that this assumption results in an upper bound on the system performance [3].

To analyze system performance under multiple user circumstance, we need the probability, p, that we will get 1 in cross-correlation between two distinct codewords at the time of detection. In other words, p is the probability that we will get a small optical pulse from an unwanted sender at the time of detection, where the power of the pulse is 1/(code weight) times of a signal pulse. Let us call p the cross-correlation probability. In the 2-D prime codes, there is one pulse per row and $p = (1/2T) \times (\text{number of rows})$ [12], [15]. In the 3-D codes with multiple (W) pulses per plane, p is given by $(1/2T) \times SW$ since the code is equivalent to the 2-D code with SW rows. In the space/wavelength/time 3-D codes w/SPP, for the pulse in a spatial channel from an unwanted sender to contribute to noise at the time of detection, it should be of the same wavelength with the pulse from the wanted sender in that spatial channel. Therefore, p is given by $(1/2T) \times (1/W) \times S$.

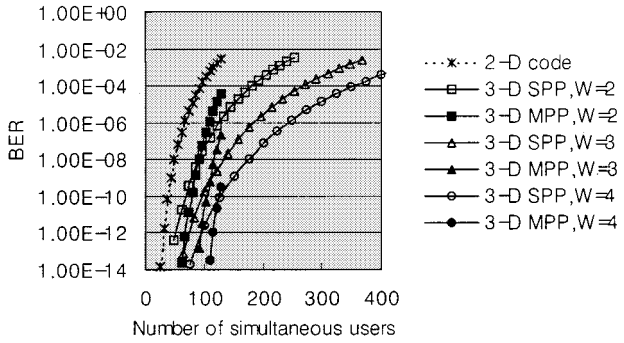

Fig. 2. Bit error rate versus the number of simultaneous users for space/wavelength/time 3-D OCDMA system and 2-D system. $S = 16$, $T = 127$, $W = 2, 3, 4$. Filled figures represent the 3-D single pulse per plane code systems and the hollow ones represent the 3-D multiple pulses per plane code systems.

Once p is given, the error probability of the system is given by

$$P_e = \frac{1}{2} \sum_{i=Th}^{N-1} \binom{N-1}{i} p^i (1-p)^{N-1-i} \tag{20}$$

where Th is a threshold in detection, N is the number of simultaneous users, and the factor 1/2 accounts for the probability that the wanted sender transmits "0" assuming equiprobable on–off data bit transmission [12], [15]. Note that when the sender transmits "1," no error occurs.

For $S = 16, T = 127$, error probabilities of the codes are calculated with various numbers of wavelength and simultaneous users by (20). In calculation, the optimal threshold, which is equal to code weight, is assumed. ($Th = S$ for 2-D code and 3-D code w/SPP, $Th = SW$ for 3-D code with W pulses per plane) Fig. 2 shows the calculated error probabilities. Both 3-D codes show the improved performance compared to the 2-D prime code. The improvement of the 3-D code w/SPP stems from the reduced cross-correlation probability, p. [Note that it is $(1/W)$ times of the cross-correlation probability of the 2-D code.] Whereas, in 3-D code w/MPP, the improvement arises from the increased threshold incurred by the increased code weight, the number of pulses in a codewords, in spite of the increased cross-correlation probability. As seen in Fig. 2, for a small number of simultaneous users, the 3-D code w/MPP shows lower error probability than the 3-D code w/SPP, which implies that the increased threshold effect is dominant. As the number of simultaneous users increases the reduced cross-correlation probability becomes dominant. Therefore, the 3-D code w/SPP shows lower error probability than the 3-D code w/MPP.

The result indicates that when we design an OCDMA system using the 3-D code with given resources (spatial channels, wavelengths, and time chips), the choice between the 3-D code w/SPP and the 3-D code w/MPP depends on the requirement of the system. For example, if 16 spatial channels and 3 wavelengths are available, and the code length is limited to 127, Fig. 2 indicates that for the system which requires bit error rate (BER) lower than 10^{-9}, the 3-D code w/MPP should be adopted. Whereas, the required BER is higher than 10^{-9}, the 3-D code w/SPP will be better choice.

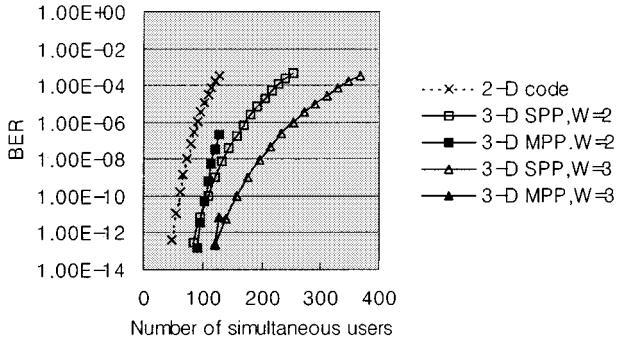

Fig. 3. Bit error rate versus the number of simultaneous users for space/wavelength/time 3-D OCDMA system and 2-D system. $S = 24$, $T = 127$, $W = 2, 3, 4$. Filled figures represent the 3-D single pulse per plane code systems and the hollow ones represent the 3-D multiple pulses per plane code systems.

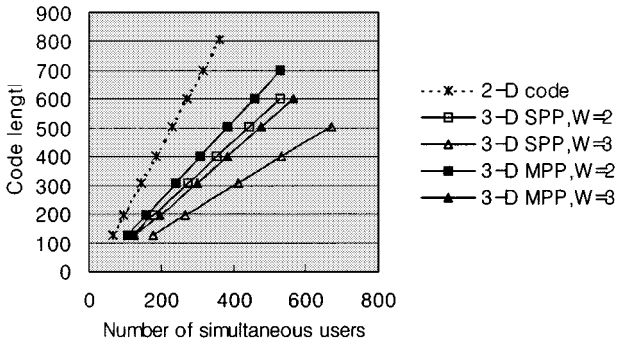

Fig. 4. Required minimum code length versus number of simultaneous users for OCDMA system based on 3-D codes and 2-D prime code with BER $= 10^{-9}$. $S = 24, W = 2, 3$. Filled figures represent the 3-D single pulse per plane code systems and the hollow ones represent the 3-D multiple pulses per plane code systems.

As the number of spatial channels increases, the range of BER where the 3-D code w/SPP outperforms the 3-D code w/MPP increases. Fig. 3 shows the calculated BER for $S = 24$, $T = 127$. Note that the crossing between the curves of the 3-D code w/SPP and the 3-D code w/MPP for $W = 2$ in Fig. 3 decreased to about BER $= 10^{-11}$, which was about BER $= 10^{-8}$ for $W = 2$ in Fig. 2. Figs. 2 and 3 also indicate that for a fixed number of spatial channels, the 3-D code w/SPP is more likely to be better choice than the 3-D code w/MPP as more wavelengths are available. This is because the maximum number of users in the 3-D code w/MPP is limited to T due to the code size limitation.

Now, let us consider the bandwidth efficiency considering the number of simultaneous users. A minimum code length required to support a number of simultaneous users with a certain BER guaranteed can be calculated. The minimum code length is limited by not only the error probability given by (20), but also the maximum number of users that is related to the code length. This implies that $P_e(N, T) \leq P_{\text{guaranteed}}$ and $N \geq T$ should be satisfied simultaneously for the 3-D code w/MPP. Fig. 4 shows the calculated minimum code length that is required to accommodate various numbers of simultaneous users with $P_e \leq 10^{-9}$ for $S = 24$, $W = 1$ (2-D code), 2, 3. As seen in Fig. 4, the 3-D codes need much shorter code lengths than the 2-D prime code in order to accommodate the same number of simultaneous users, which means larger per-user bandwidth is provided by using the 3-D codes. In Fig. 4, the 3-D codes w/SPP show reduction in the code size approximately by the factor of $1/W$ compared with the 2-D prime code, which implies increase in the per-user bandwidth by the factor of W. One can see that the improved error probability behavior of the 3-D codes brings about the much improved bandwidth efficiency.

In Fig. 4, one can also see that the 3-D code w/SPP outperforms the 3-D code w/MPP for the given conditions. However, as mentioned previously, it should be stressed that the 3-D code w/MPP can be better choice than the 3-D code w/SPP depending on the error probability requirement of the system. If the required BER is much lower than 10^{-9}, the situation could be different. Nevertheless, we would like to point out that as available spatial channels and wavelengths increase, the 3-D code w/SPP will be more likely to show better performance.

C. Scalability of OCDMA System

Another measure of the OCDMA system is scalability of the system, that is, how easily the number of simultaneous users can be increased with minimum modification of network configuration. The number of codewords in the 3-D code w/MPP is limited by the code length T, whereas that in the 3-D code w/SPP is WT assuming $W < S$. The number of codewords of the 3-D code w/MPP does not change as the number of wavelength increases. As a result, when we need to increase the number of simultaneous users with the same BER guaranteed for a deployed system, we can accommodate more users by employing more wavelengths in the systems based on the 3-D code w/SPP, whereas we cannot accommodate more than T simultaneous users in the systems base on the 3-D code w/MPP no matter how many wavelengths are employed. For example, let us consider the systems composed of $S = 16$, $W = 3$, $T = 127$ with BER equal to 10^{-9}. According to Fig. 2, both systems based on the 3-D code w/SPP and the 3-D code w/MPP can accommodate roughly 100 simultaneous users. By employing another wavelength, the number of simultaneous users can be increased to about 150 and 127 with BER $\leq 10^{-9}$ in the systems of the 3-D code w/SPP and the 3-D code w/MPP, respectively. If more wavelengths are available, we can accommodate more simultaneous users in the systems of the 3-D code w/SPP. By contrast, in the systems of the 3-D code w/MPP, the number of simultaneous users is now limited by the number of codewords (code set size) and we cannot accommodate more than 127 users even if more wavelengths are used. All the effect of increased wavelengths on the system is to reduce BER in that case. Therefore, it can be said that the 3-D code w/SPP has greater system scalability than the 3-D code w/MPP.

Another advantage of the OCDMA system based on the 3-D code w/SPP is that adding wavelengths does not affect the existing users or network configuration at all. Only the new users need to be equipped with encoders/decoders that can process the added wavelengths, which also offers great system extendibility.

Before closing this section, we would like to point out that the basic concept of the WDM/CDMA hybrid schemes suggested in [17]–[21] is equivalent to the code w/SPP proposed in this paper, and with the WDM/CDMA hybrid schemes, 3-D orthogonal codes that have similar performance to the 3-D code w/SPP can be constructed if the compete set of orthogonal codewords

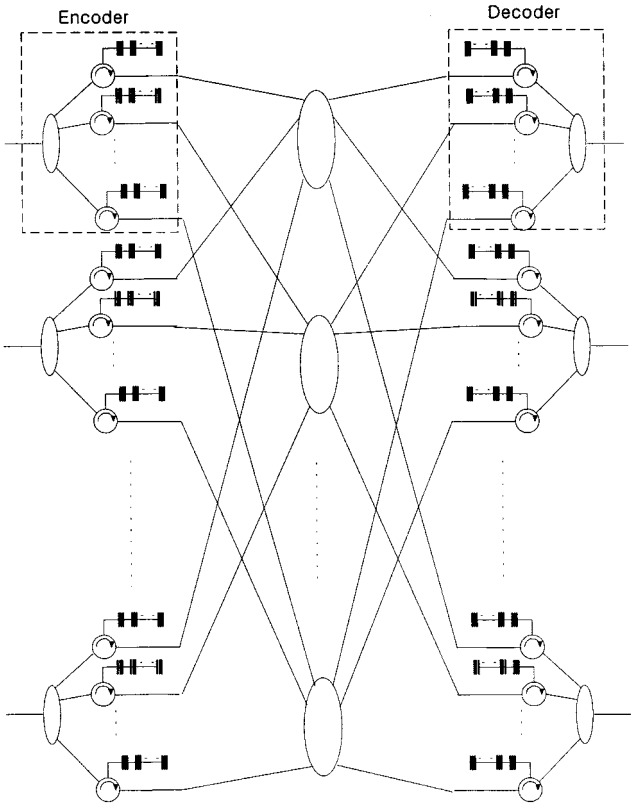

Fig. 5. Structure of space/wavelength/time 3-D OCDMA networks. (Multiple pulses per plane case. For case of single pulse per plane, only one fiber grating is used in each spatial channel.)

can be found. One of the hybrid schemes that was referred to as the WDM matrix code in [18] appears to have larger code set size which is proportional to $W!$, but this is the result of the loose cross-correlation constraint as mentioned earlier. Although only orthogonal 3-D codes are considered in this work, the compromise between the cross-correlation value and the system performance to increase the code set size may be an interesting research topic. This remains as one of a number of directions for further research at this time.

VI. Implementation of 3-D Code and Wavelength^2/Time Scheme

Structures of OCDMA systems based on 3-D codes are discussed in this section. Fig. 5 depicts the general configuration of the OCDMA system based on the space/wavelength/time 3-D code w/MPP. Each fiber connecting the encoder/decoder and the star coupler corresponds to each spatial channel and the center wavelength each fiber grating is tuned to each wavelength of the code. An optical pulse, which has broadband spectrum, incident into the encoder is split into the circulators, and each wavelength component of the optical pulse is reflected at the fiber grating of different location. As a result, we obtain a series of optical pulses with different wavelength components in each fiber. In the decoder, if the sequence and the relative distances among the fiber gratings are properly determined, the series of optical pulses are assembled in the same time chip obtaining one large optical pulse. The system of the 3-D code w/SPP is of similar configuration to Fig. 5. Only the difference is that there is one

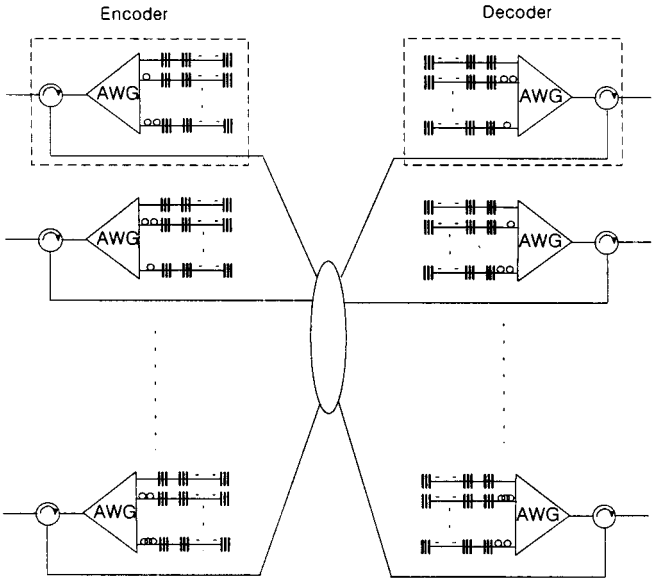

Fig. 6. Structure of wavelength^2/time implementation of the 3-D OCDMA networks. Center wavelengths of the fiber gratings connected to an output port of AWG's in the encoder/decoder are separated by free spectral range of AWG.

fiber grating in each spatial channel of the encoder/decoder. The length of each delay line, the relative distances among gratings, and the center wavelength of each grating are determined by a corresponding codeword given in Section IV. In the structure shown in Fig. 5, the path length of each spatial channel between a pair of encoder and decoder should be same. Otherwise, all the spread pulses will not be collected in the same time chip at the intended receiver and thus, error occurs. However, it is very difficult to realize. Although the difficulty can be partially relaxed by use of fiber ribbons, requirement of multiple star couplers is also disadvantageous. To make the 3-D code more feasible, we need to eliminate the requirement of fiber ribbons and multiple star couplers.

The reason that we need multiple star couplers in the structure shown in Fig. 5 is to prevent optical pulses in different spatial channels from being mixed together before correlated. If we assign different sets of wavelengths, $\{\lambda_{s,w}\}$, to spatial channels, s, we do not need multiple star couplers. In this scheme, the pulse of λ_w in spatial channel s replaced with a pulse of $\lambda_{s,w}$, and we can send pulses of all spatial channels though one fiber without mixing. As a result, the requirement of multiple star couplers is eliminated. As it were, space/wavelength/time 3-D code is converted to wavelength^2/time code for implementation. This scheme can be easily implemented with help of periodic characteristics of $1 \times S$ AWG [22]. When a number of wavelengths are demultiplexed in an AWG, a group of wavelengths which are separated by free spectral range of the AWG are coupled into the same output port. Therefore, if we assign the group of wavelengths to a spatial channel, the scheme can be implemented by the structure shown in Fig. 6. As seen in Fig. 6, each output port of the AWG in the encoder/decoder corresponds to a spatial channel in the space/wavelength/time 3-D code, and the center wavelengths of gratings in each fiber belong to a group of wavelengths that can be coupled to the corresponding output port of the AWG. Fig. 6 depicts the structure

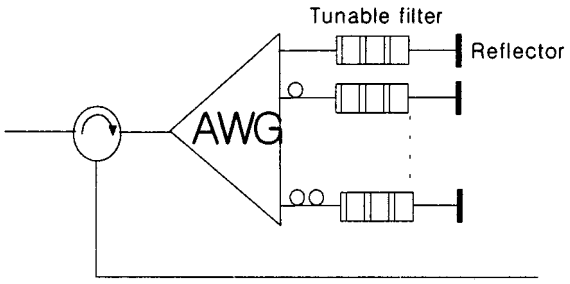

Fig. 7. Structure of encoder/decoder for wavelength^2/time OCDMA networks with tunable filters and reflectors. By employing tunable filters, many codewords can be encoded/decoded selectively with a encoder/decoder.

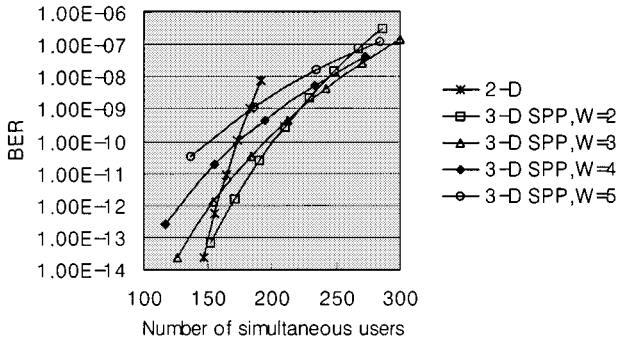

Fig. 8. Bit error rate versus the number of simultaneous users for single pulse per plane wavelength^2/time 3-D OCDMA system and 2-D system with 60 wavelengths. $W' = 60$, $T = 197$, $W = 2, 3, 4, 5$. (The 3-D OCDMA systems with multiple pulses per plane for various W show the same BER with that of the 2-D system if the number of total available wavelengths is fixed.)

for wavelength^2/time scheme for the 3-D code w/MPP. We can implement wavelength^2/time scheme for the 3-D code w/SPP by using only one grating in each output of the AWG in encoder/decoder. In either structure, lengths of delay lines between gratings and the order of gratings are determined according to the 3-D codes given in Section IV.

Note that in structures shown in Figs. 5 and 6, we do not need coherent light sources such as laser diodes (LD's). Instead of a bunch of LD's, one incoherent broadband light source such as light emitting diode (LED) is used for each user, which is advantageous over wavelength division multiple access system. Within the bandwidth of the light source, we can increase the number of wavelengths by simply increasing the number of the AWG ports or employing more kinds of fiber gratings.

The wavelength^2/time scheme w/MPP is equivalent to ($W' \times T$, W', 0, 1) wavelength/time 2-D code, where $W' = SW$, in the aspect of code construction and error probability if $S > W$. The advantage of the wavelength^2/time scheme is that an AWG with a smaller number of ports is used in the implementation of the codes. Note that $1 \times W'$ AWG's are needed to implement ($W' \times T$, W', 0, 1) wavelength/time 2-D code, while $1 \times S$ AWG's are needed for wavelength^2/time scheme. Moreover, if the wavelength^2/time scheme w/SPP is employed, we will have system extendibility and can accommodate more simultaneous users depending on system requirements as discussed previously. Another advantage of the wavelength^2/time scheme w/SPP is that if we use tunable filters and reflectors instead of fiber gratings as depicted in Fig. 7, W codewords (when $S > W$) or W^2 codewords (when $S \leq W$) can be selectively transmitted or received with one encoder/decoder by tuning the filters.

To compare the performance of the wavelength^2/time scheme w/SPP with that of 2-D code or wavelength^2/time scheme w/MPP, the error probability of ($W' \times T$, W', 0, 1) 2-D wavelength/time code system and [$(W'/W) \times W \times T$, (W'/W), 0, 1] wavelength^2/time scheme w/SPP for various W are calculated assuming the total number of available wavelengths is fixed to W'. Note that the performance of [$(W'/W) \times W \times T$, W', 0, 1] wavelength^2/time scheme w/MPP is the same with that of ($W' \times T$, W', 0, 1) 2-D wavelength/time code system. Fig. 8 shows the calculated result for $W' = 60$, $T = 197$. If the required BER is higher than 10^{-9}, ($20 \times 3 \times 197$, 20, 0, 1) wavelength^2/time scheme w/SPP shows best performance. For the system which requires BER lower than 10^{-9}, ($30 \times 2 \times 197$, 30, 0, 1) wavelength^2/time scheme w/SPP is the best choice. This result indicates that OCDMA system performance can be maximized for a given number of wavelengths and a given code length by employing the wavelength^2/time scheme.

VII. Conclusion

In this paper, we constructed space/wavelength/time spread 3-D optical orthogonal codes by extending the 2-D prime codes, and the performance of 3-D codes are analyzed and compared to that of the 2-D code. The 3-D codes showed much improve performance compared to the 2-D prime code. In construction of the 3-D codes, we proposed two types of codes with different numbers of pulses per wavelength/time plane, the 3-D codes w/SPP and the 3-D codes w/MPP, and investigated the effect of the number of pulses per wavelength/time plane on performance. For a small number of simultaneous users, the 3-D code w/MPP showed better performance due to dominant effect of increased threshold. The 3-D code w/SPP showed lower error probability for a large number of simultaneous users since the effect of reduced cross-correlation probability became dominant. This implies that the choice between the two 3-D codes depends on the amount of traffic in the access networks. Physical implementations of the proposed 3-D codes were also considered. To eliminate the requirement of fiber ribbons and multiple star couplers for implement of space/wavelength/time codes, we proposed the wavelength^2/time scheme in which the periodic property of an AWG is used. The performance of the wavelength^2/time scheme w/SPP was compared to the 2-D prime code system with the same number of wavelengths for fair comparison. It was shown that the wavelength^2/time scheme w/SPP could accommodate more users depending on the system requirement. We believe that the proposed wavelength^2/time scheme w/SPP enhanced the feasibility and the scalability of OCDMA system based on the 3-D codes.

In this paper, only the prime code algorithm was considered for 2-D and 3-D code construction, but we would like to point out that all the ideas for the extension of 2-D code to 3-D code and the wavelength^2/time scheme are still valid for the Reed–Solomon code algorithm.

REFERENCES

[1] F. R. K. Chung, J. A. Salehi, and V. K. Wei, "Optical orthogonal codes: Design, analysis, and applications," *IEEE Trans. Inform. Theory*, vol. 35, pp. 595–604, May 1989.

[2] J. A. Salehi, "Code division multiple access techniques in optical fiber networks—Part I: Fundamental principles," *IEEE Trans. Commun.*, vol. 37, pp. 824–833, Aug. 1989.

[3] J. A. Salehi and C. A. Brackett, "Code division multiple access techniques in optical fiber networks—Part II: System performance analysis," *IEEE Trans. Commun.*, vol. 37, pp. 834–850, Aug. 1989.

[4] H. Chung and P. V. Kumar, "Optical orthogonal codes—New bounds and an optimal construction," *IEEE Trans. Inform. Theory*, vol. 36, pp. 866–873, July 1990.

[5] A. A. Shaar and P. A. Davies, "Prime sequences: Quasi optimal sequences for channel code division multiplexing," *Electron. Lett.*, vol. 19, pp. 888–889, Aug. 1989.

[6] A. S. Holmes and R. R. Syms, "All optical CDMA using quasi prime code," *J. Lightwave Technol.*, vol. 10, pp. 279–286, Feb. 1992.

[7] S. V. Maric, Z. I. Kostic, and E. L. Titelbaum, "A new family of optical orthogonal sequences for use in spread spectrum fiber optic local area networks," *IEEE Trans. Commun.*, vol. 41, pp. 1217–1221, Aug. 1993.

[8] S. V. Maric, "New family of algebraically designed optical orthogonal codes for fiber optic CDMA networks," *Electron. Lett.*, vol. 29, pp. 538–539, Mar. 1993.

[9] F. J. MacWilliams and N. J. A. Sloane, *The Theory of Error-Correcting Codes*. Amsterdam, The Netherlands: North-Holland, 1986.

[10] G.-C. Yang and J.-Y. Jaw, "Performance analysis and sequence designs of synchronous code-division multiple access systems with multi-media services," in *Proc. Inst. Elect. Eng.-Communications*, Dec. 1994, vol. 141, pp. 371–378.

[11] E. Park, A. J. Mendez, and E. M. Garmire, "Temporal/spatial optical CDMA networks: Design, demonstration and comparison with temporal network," *IEEE Photon. Technol. Lett.*, vol. 4, pp. 1160–1162, Oct. 1992.

[12] E. S. Shivaleela, K. N. Sivarajan, and A. Selvarajan, "Design of new family of two-dimensional codes for fiber-optic CDMA networks," *J. Lightwave Technol.*, vol. 16, no. 4, pp. 501–508, Apr. 1998.

[13] A. J. Mendez, J. L. Lambert, J.-M. Moroonkian, and R. M. Gargliadi, "Sythesis and demonstrated high speed, bandwidth efficient optical code division multiple access (CDMA) tested at 1 Gb/s throughput," *IEEE Photon. Technol. Lett.*, vol. 6, pp. 1146–1149, 1994.

[14] L. Tancevski and I. Andonovic, "Wavelength hopping/time spreading code division multiple access systems," *Electron. Lett.*, vol. 30, no. 17, pp. 1388–1390, 1994.

[15] G.-C. Yang and W. C. Kwong, "Performance comparison of multiwavelength CDMA and WDMA + CDMA for fiber-optic networks," *IEEE Trans. Commun.*, vol. 45, no. 11, pp. 1426–1434, Nov. 1997.

[16] T. Pfeiffer, B. Deppisch, M. Witte, and R. Heidemann, "Optical stability of a spectrally encoded optical CDMA system using inexpensive transmitters without spectral control," *IEEE Photon. Technol. Lett.*, vol. 11, pp. 916–918, 1999.

[17] A. J. Mendez and R. M. Gagliardi, "Code division multiple access (CDMA) enhancement of wavelength division multiple access (WDM) systems," in *IEEE Int. Conf. Commun. (ICC'95)*. Seattle, WA, 1995, paper 8.3, pp. 271–276.

[18] A. J. Mendez, "WDM Matrix coding: A novel approach to ultra-dense networks," in *WDM Components Conf., Photon. West'96*, vol. 2690, 1996, pp. 50–62.

[19] R. M. Gagliardi and A. J. Mendez, "Performance improvement with hybrid WDM and CDMA optical communications," in *Proc. WDM Components Conf., Photon.s West'96*, vol. 2690, 1996, pp. 88–96.

[20] A. J. Mendez and R. M. Gagliardi, "Varieties and characteristics of discrete spectral encoding (DSE)," in *Proc. IEEE 4th Int. Symp. Spread Spectrum Techniques Appl. (ISSSTA'96)*, 1996, IEEE Conf. Proc. 96TH8210, pp. 438–444.

[21] ——, "Design and analysis of wavelength division multiplex (WDM) and code division multiple access (CDMA) hybrids (WCH)," in *Proc. IEEE/LEOS'96*, 1996, paper WX4, pp. 185–186.

[22] H. Takahashi, K. Oda, H. Toba, and Y. Inoue, "Transmission characteristics of arrayed waveguide $N \times N$ wavelength multiplexer," *J. Lightwave Technol.*, vol. 13, pp. 447–455, Mar. 1995.

Sangin Kim was born in Seoul, Korea in 1971. He received the B.S. degree in electrical engineering from the Korea Advanced Institute of Science and Technology (KAIST), Taejeon, Korea in 1992. He received the M.S. and Ph.D. degrees in electrical engineering from the University of Minnesota, Minneapolis–St. Paul, MN, in 1995 and 1997, respectively.

He joined Korea Telecom in 1997, and since then, he has been involved in development of high-capacity optical switching systems. Currently, he is working on design and implementation of optical subscriber access networks. His research interests cover a broad spectrum of photonic and electrooptic device physics, guided-wave optics, photonic nanostructures, and photonic integrated circuits.

Kyungsik Yu was born in Inchon, Korea, on May, 17, 1977. He received the B.S. degree in electrical engineering from Seoul National University, Seoul, Korea, in 1999. He is currently working towards the M.S. and Ph.D. degrees in electrical engineering at Stanford University, Stanford, CA.

His research interests include optical CDMA and coding, and free-space communication using grating light valve and digital image and video watermarking.

Namkyoo Park (S'90–M'94) received the B.S. and M.S. degrees from Seoul National University, Seoul, Korea, in 1987 and 1988, respectively, and Brown University, Providence, RI, in physics. He received the Ph.D. degree in applied physics from the California Institute of Technology, Pasadena, CA, in 1994

He was with AT&T Bell Laboratories, Murray Hill, NJ, as a Postdoctoral Fellow. From 1996 to 1997, he participated in the development of high-capacity optical transmission systems in Samsung Electronics, and is currently working as an Assistant Professor in the School of Electrical Engineering and Computer Science in Seoul National University. He has authored and coauthored more than 30 international papers in international journals, and presented results at over 40 international conferences. His current research interests include wideband optical amplifiers, amplifier transient dynamics, duo-binary transmission, soliton control, and optical CDMA for those he holds five international and 12 domestic patents.

Dr. Park is a member of the Optical Society of America (OSA) and currently working as a General Affair Secretariat for Optical Society of Korea.